THE JOURNAL OF PHYSICAL CHEMISTRY Letters

Cite This: J. Phys. Chem. Lett. 2019, 10, 1935−1941

Letter

pubs.acs.org/JPCL

Ion Mobility-Mass Spectrometry of Iodine Pentoxide−Iodic Acid Hybrid Cluster Anions in Dry and Humidified Atmospheres

Lauri Ahonen,[†] Chenxi Li,[‡,§] Jakub Kubečka,[†] Siddharth Iyer,[∥] Hanna Vehkamäki,[†] Tuukka Petäjä,[†] Markku Kulmala,[†] and Christopher. J. Hogan Jr*[,‡]

[†]Institute for Atmospheric and Earth System Research/Physics, Faculty of Science, University of Helsinki, FI-00014 Helsinki, Finland

[‡]Department of Mechanical Engineering, University of Minnesota, Minneapolis, Minnesota 55455, United States

[§]Laboratory for Physical Chemistry, ETH Zürich, 8093 Zürich, Switzerland

[∥]Institute for Atmospheric and Earth System Research/Chemistry, University of Helsinki, P.O. Box 55, FI-00014 Helsinki, Finland

Supporting Information

ABSTRACT: Nanometer-scale clusters form from vapor-phase precursors and can subsequently grow into nanoparticles during atmospheric nucleation events. A particularly interesting set of clusters relevant to nucleation is hybrid iodine pentoxide−iodic acid clusters of the form $(I_2O_5)_x(HIO_3)_y$ as these clusters have been observed in coastal region nucleation events in anomalously high concentrations. To better understand their properties, we utilized ion mobility-mass spectrometry to probe the structures of cluster anions of the form $(I_2O_5)_x(HIO_3)_y(IO_\alpha)^-$ (x = 0−7, y = 0−1, α = 1−3), similar to those observed in coastal nucleation events. We show that $(I_2O_5)_x(HIO_3)_y(IO_\alpha)^-$ clusters are relatively stable against dissociation during mass spectrometric measurement, as compared to other clusters observed in nucleation events over continental sites, and that at atmospherically relevant relative humidity levels (65% and less) clusters can become sufficiently hydrated to facilitate complete conversion of iodine pentoxide to iodic acid but that water sorption beyond this level is limited, indicating that the clusters do not persist as nanometer-scale droplets in the ambient.

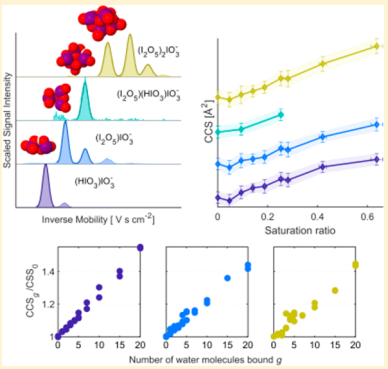

Atmospheric nucleation events occur when vapor-phase precursors bind to one another, forming stable, condensed-phase molecular clusters.[1−3] Though considerable progress has been made in understanding atmospheric nucleation via a combination of field measurements, laboratory experiments, and computational models,[4−11] prediction of nucleation rates and construction of accurate cluster to nanoparticle growth models both remain difficult. This is in large part because the physicochemical properties of nucleation event-formed clusters, which determine both their stability and their potential for subsequent growth, have not been fully characterized. Limitations in signal intensity and in cluster lifetime in the ambient typically prohibit in situ characterization beyond chemical identification.

There is therefore interest in greater characterization of the stability, structure, and hydration (as clusters in the ambient are in frequent contact with water) of clusters identified as forming during atmospheric nucleation events. A particularly pertinent, yet relatively unstudied, class of clusters are iodine pentoxide−iodic acid hybrid clusters of the form $(I_2O_5)_x(HIO_3)_y$. These clusters have been observed to form from biogenic iodine precursors during nucleation events in coastal regions,[12−16] wherein the cluster formation and growth rates are anomalously high[17] in comparison to continental nucleation events. In this study, we have utilized ion mobility-mass spectrometry (IM-MS,[18] with a high-resolution differential mobility analyzer coupled to a mass spectrometer[19]) to measure the collision cross sections (CCSs) of cluster anions of the form $(I_2O_5)_x(HIO_3)_y(IO_\alpha)^-$ with x = 0−7, y = 0−1, and α = 1−3. In using IM-MS as a cluster characterization technique, we follow the methods outlined by Oberreit et al.[20] and Thomas et al.,[21] with three specific objectives: (1) we assess relative cluster ion stability by monitoring dissociation between atmospheric-pressure mobility measurements and low-pressure mass spectrometry measurements; (2) we compare the CCSs, which were measured in CO_2, to CCS predictions based on both specular and diffuse gas molecule scattering predictions with all-atom cluster models;[22,23] and (3) we examine CCS shifts in the presence of water vapor (near 295 K, at saturation ratios of up to 0.65).

Differential mobility analysis-mass spectrometer measurements were performed on electrospray-generated cluster anions (using 1 mM iodic acid in HPLC water), with additional details on measurements provided in the Supporting

Received: February 16, 2019
Accepted: April 2, 2019
Published: April 2, 2019

DOI: 10.1021/acs.jpclett.9b00453
J. Phys. Chem. Lett. 2019, 10, 1935−1941

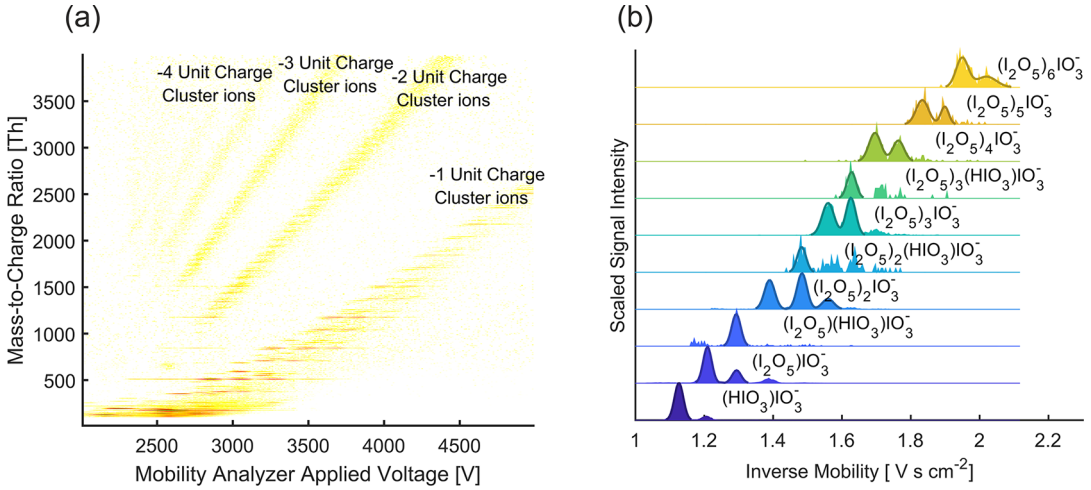

Figure 1. (a) Contour plot of the measured signal intensity as a function of the mass-to-charge ratio and mobility analyzer applied voltage for electrospray-generated cluster anions. (b) Post-calibration inverse mobility spectra for specific mass-identified cluster anions. The chemical compositions of the selected ions are noted.

Information. In using electrospray ionization to generate clusters, we assume that the clusters formed for a given chemical composition adopt structures similar to those generated during atmospheric nucleation, i.e., clusters "equilibrate" to conformations that are not dependent on their formation process. Measurements result in detected ion signal as a function of mass-to-charge ratio and the applied differential mobility analyzer voltage, which is convertible to inverse mobility after instrumentation calibration.[24,25] Contour plots of raw data for cluster ions with mobility measurements made in dry CO_2 at 295 K (with immeasurably low water content, below 1% relative humidity) are shown in Figure 1a. Signal corresponding to ions of a specific composition and specific structure take the form of "line segments", and line segments are grouped by charge state. We focus solely on the singly charged cluster ions in this study as multiply charged clusters are generally unique to electrospray ionization and are unlikely to be observed in atmospheric nucleation events. For selected singly charged cluster ions where the excess charge is carried by the IO_3^- ion, post-calibration inverse mobility spectra are provided in Figure 1b. Evident in the figure, for all ions, there are multiple peaks detected. In many instances, peaks of "neighboring" cluster ions, i.e., cluster ions with compositions differing by a single iodine pentoxide (I_2O_5) or iodic acid (HIO_3) or with I_2O_5 displaced by HIO_3, coincide exactly with one another in location. In IM-MS measurements, this is known to arise because of either dissociation reactions (i.e., $(I_2O_5)_x(HIO_3)_y(IO_3)^- \rightarrow (I_2O_5)_{x-1}(HIO_3)_y(IO_3)^- + I_2O_5$ and $(I_2O_5)_x(HIO_3)(IO_3)^- \rightarrow (I_2O_5)_x(IO_3)^- + HIO_3$) or displacement reactions (the reaction $(I_2O_5)_x(IO_3)^- + H_2O \rightarrow (I_2O_5)_{x-1}(HIO_3)(IO_3)^- + HIO_3$ in this instance) after mobility measurement but prior to mass measurement.[26] Signal appears in such instances at the inverse mobility of the parent ion but the mass-to-charge ratio of the product ion. For all detected clusters ions, the peaks of the smallest inverse mobilities can be identified as arising from unreacted parent ions. However, for all cluster ions smaller than $(I_2O_5)_4IO_3^-$, the secondary and tertiary peaks at higher inverse mobilities clearly align with peaks in the inverse mobility spectra of higher mass ions; this suggests that they arise from dissociation or displacement reactions. For $(I_2O_5)_xIO_3^-$ with x = 4−7 (with the spectrum for x = 7 not shown), secondary inverse mobility peaks are apparent, yet these peaks do not coincide with peaks in the spectra of larger ions. They are likely indicative of a second, unique structure type adopted by larger cluster ions that does not interconvert with the lower inverse mobility structure type during measurement.

The differential mobility analyzer-mass spectrometer system employed has been utilized under identical measurement conditions (including inlet voltage settings) to analyze a variety of other cluster ions. The extent of dissociation reactions observed here can be compared to these prior results and hence used to qualitatively assess the stability of hybrid iodine pentoxide−iodic acid cluster ions. Ouyang et al.[27] examined positively charged alkali metal iodide cluster ions of the form $(XI)_nX^+$ (X = Na, K, Rb, Cs and n = 1−13), and Thomas et al.[21] examined positively and negatively charged hybrid dimethylammonium bisulfate−sulfuric acid cluster ions with up to eight dimethylammonium bisulfate ion pairs and three sulfuric acid molecules (which are similar in composition to those detected in atmospheric nucleation events in a number of continental sites).[5−7,28,29] In both of these prior studies, multiple successive dissociation reactions were observed to take place subsequent to mobility analysis and prior to mass analysis; for positively charged dimethylammonium bisulfate−sulfuric acid cluster ions, dissociation was often severe enough to leave parent ions undetectable. The extent of dissociation and displacement reaction observed for iodine pentoxide−iodic acid hybrid clusters is much smaller than that observed in prior studies of other cluster ion types. They can thus be regarded as a particularly stable class of cluster anions compared to those studied previously via atmospheric-pressure IM-MS. We postulate that their high levels of stability may contribute to the high nucleation rates observed when such clusters form as when dissociation is minimal the nucleation rate can approach a collision-controlled limit.[30,31]

More direct than stability, IM-MS measurements yield the CCSs of the identified cluster ions via application of the Mason−Schamp equation (the equation linking mobility/diffusivity to CCS).[32] By comparing measurement results to predictions of CCSs based on computationally derived structures, we can assess to what extent computationally modeled structures capture the global structural features of clusters. In the experiment−model comparison, we considered

DOI: 10.1021/acs.jpclett.9b00453
J. Phys. Chem. Lett. 2019, 10, 1935−1941

Table 1. Summary of the Cluster Formulas, Masses, Measured CCSs, and Predicted CCSs Using the EHSS and DHSS Calculation Approaches[a]

molecular formula	mass [Da]	CCS [Å^2]	N	EHSS [Å^2]		DHSS [Å^2]	
$(HIO_3)_1IO_2^-$	334	187 ± 4	0				
$(HIO_3)_1IO_3^-$	350	186 ± 3	2	129	129	179	179
$(I_2O_5)_1IO^-$	476	197 ± 3	2	138	141	190	194
$(I_2O_5)_1IO_2^-$	492	205 ± 4	2	139	141	190	192
$(I_2O_5)_1IO_3^-$	508	204 ± 3	2	140	143	193	194
$(HIO_3)_2IO_2^-$	510	203 ± 3	0				
$(I_2O_5)_1(HIO_3)IO_3^-$	684	220 ± 3	2	153	155	211	213
$(I_2O_5)_2IO_2^-$	826	234 ± 3	1	185		243	
$(I_2O_5)_2IO_3^-$	842	238 ± 4	1	164	162	223	223
$(I_2O_5)_2(HIO_3)IO_3^-$	1018	255 ± 3	1	196		259	
$(I_2O_5)_3IO_2^-$	1160	265 ± 4	1	192		259	
$(I_2O_5)_3IO_3^-$	1176	269 ± 4	2	185	194	249	257
$(I_2O_5)_3(HIO_3)IO_3^-$	1352	281 ± 3	1	210		279	
$(I_2O_5)_4IO_2^-$	1494	295 ± 11	0				
$(I_2O_5)_4IO_3^-$	1510	293 ± 4	2	225	212	294	281
$(I_2O_5)_3(HIO_3)_3IO_3^-$	1703	314 ± 6	0				
$(I_2O_5)_5IO_3^-$	1843	318 ± 4	2	232	217	307	290
$(I_2O_5)_6IO_3^-$	2177	339 ± 4	2	249	256	327	336
$(I_2O_5)_7IO_3^-$	2511	365 ± 4	1	284		369	

[a]N is the number of candidate cluster structures, with the predicted CCSs shown for each candidate.

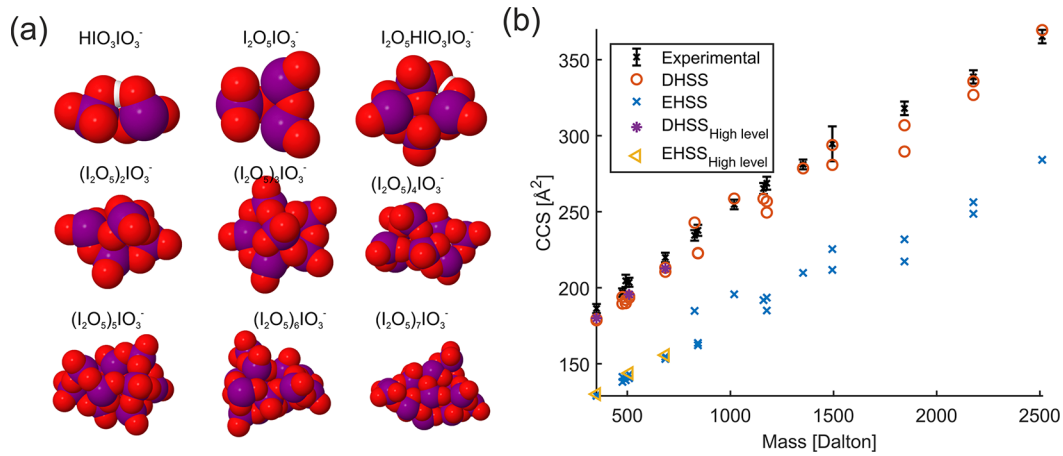

Figure 2. (a) Depictions of selected cluster ion candidate structures. Purple: iodine atoms. Red: oxygen atoms. (b) Experimentally inferred and calculated CCSs as a function of cluster ion mass. The subscript "High level" refers to structures obtained from DFT (ωB97xD//aug-cc-pVTZ-PP level) using a sufficiently large basis set. Error bars are based on the uncertainty in the mobility analyzer voltage corresponding to the peak signal intensity.

only the CCSs of ions based on the primary peak (lowest inverse mobility) in each inverse mobility spectrum as we are confident that these peaks do not arise from postmobility analyzer dissociation or displacement reactions. Experimentally inferred CCSs for these ions are noted in Table 1. Candidate cluster structures for CCS calculations were generated as described in the Supporting Information. Briefly, for the clusters $(HIO_3)IO_3^-$, $(I_2O_5)IO_3^-$, and $(I_2O_5)(HIO_3)IO_3^-$, structures were optimized using density functional theory (DFT) at the ωB97xD//aug-cc-pVTZ-PP level. For larger clusters, cluster structures were identified by first determining the partial atomic charges extracted for each of the iodine-containing monomer acids, oxides, and anions (i.e., HIO_3, I_2O_5, and IO_3^-) in cluster ions by running a single-point population analysis calculation and then using partial charges in configurational sampling via the Artificial Bee Colony (ABC) algorithm[33] with rigid molecules to construct clusters, which were again reoptimized with a low DFT level of theory. To compute CCSs, we utilized IMoS,[22,23] considering the ion-induced dipole potential between impinging CO_2 molecules and clusters[34,35] but treating atoms as hard spheres, considering both elastic hard-sphere scattering (EHSS) and diffuse hard-sphere scattering (DHSS) models. In the EHSS model, gas molecule collisions are modeled as elastic and specular (translational kinetic energy is conserved), while in the DHSS model, gas molecules are re-emitted from the ion surface at a diffuse angle (randomly selected) upon impingement on the ion surface and the gas molecule's velocity is resampled from a modified Maxwell–Boltzmann distribution.[22] Discussed previously,[27,36] for nanometer-scale ions, these two scattering models lead to appreciable differences in CCS predictions (as much as 30% in many instances), and for polyatomic gas molecules such as CO_2, we expect that the DHSS model should more accurately describe the gas

DOI: 10.1021/acs.jpclett.9b00453
J. Phys. Chem. Lett. 2019, 10, 1935−1941

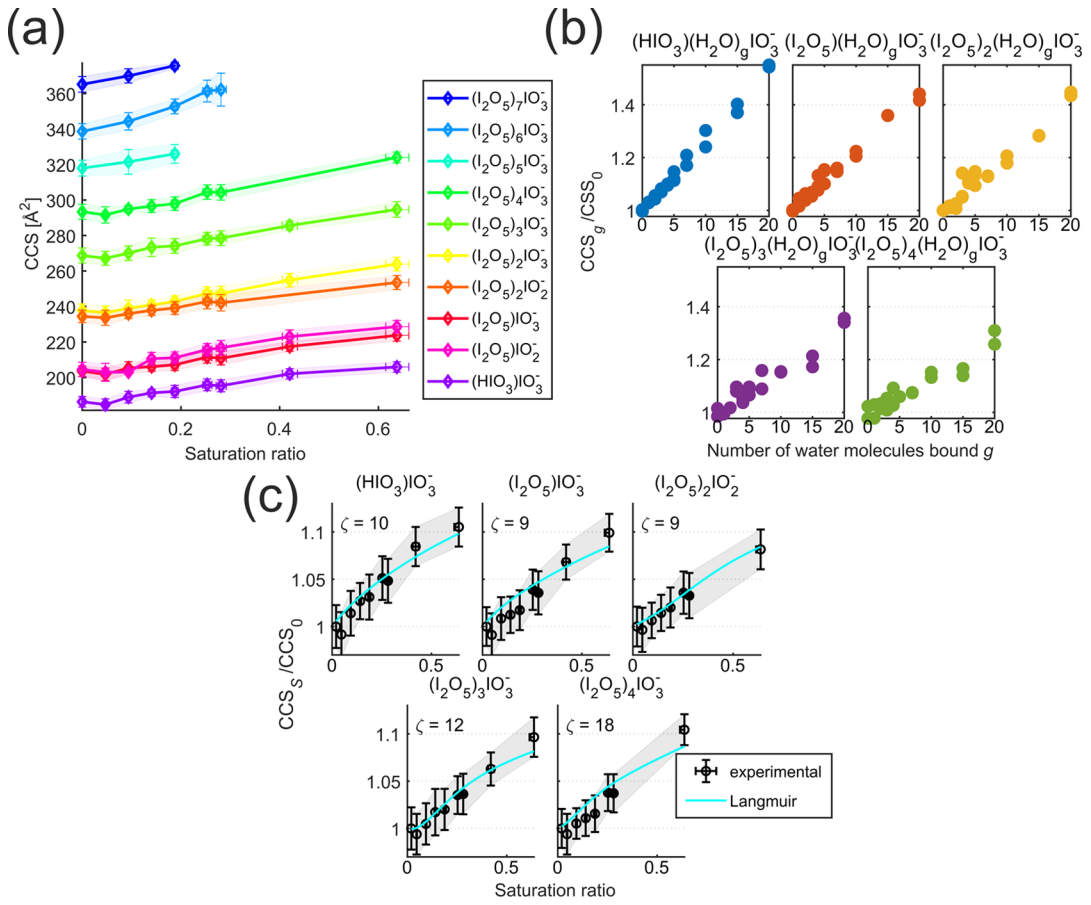

Figure 3. (a) Measured CCS as a function of saturation ratio. (b) Computed ratio CCS_g/CCS_0 as function of the number of water molecules (g) bound to a cluster ion. (c) Comparison of the CCS given by the Langmuir model fitted to experimental data for five selected cluster ions. The value of the fitting parameter ζ, the maximum number of water molecules that can bind to each cluster, is noted. Error bars are based on the uncertainty in the mobility analyzer voltage corresponding to the peak signal intensity.

molecule scattering process on an ion modeled as frozen (fixed) during calculation.[27,35−37]

Predicted CCSs based on the two models are shown in Table 1 for direct comparison to experimentally inferred values. Depictions of the cluster ion structures employed in calculations (for selected clusters) are shown in Figure 2a, and a plot of measurement inferred and calculated CCSs as a function of cluster ion mass is shown in Figure 2b. Calculation results are shown for multiple potential cluster ion structures. Consistent with prior studies on the influence of cluster structure on the CCS,[38] differences in the predicted CCSs for different structures are significantly smaller than the influence of the scattering model. Results show clearly that DHSS model predictions are in good agreement with measurements. Noteworthy about this is that neither candidate structure characterization nor CCS calculations utilized input parameters that were "fit" to measurements, and it demonstrates that both the higher-level and lower-level computations of cluster ion structures accurately capture global structure features of clusters.

Prior work has shown that by adding condensable vapor in mobility analyzers the sorption/binding of vapor can be examined at the molecular level as binding, even transiently, leads to detectible mobility/CCS shifts.[20,39,40] For iodine pentoxide−iodic acid hybrid clusters, the sorption of water vapor is of particular interest as water facilitates the interconversion of iodine pentoxide and iodic acid.[41,42] We examined water vapor sorption at 295 K and saturation ratios from 0.0 to 0.65 by monitoring CCS shifts for the cluster ions $(HIO_3)IO_3^-$ and $(I_2O_5)_xIO_3^-$ ($x = 1 - 7$). Figure 3a displays a plot of the CCS as a function of saturation ratio. It is evident in the figure that CCSs for all cluster ions measured increase noticeably but by less than 12% over the saturation ratio range examined. This is a clear indication of water vapor sorption but not to the extent wherein cluster ions would sorb sufficient quantities of water to behave as nanometer-scale droplets (i.e., where clusters, by volume, are largely composed of condensing solvent, as has been observed for cluster ions exposed to some organic species).[43] We can additionally compare the extent of observed CCS shifts to the computed change in CCS associated with the sorption of water vapor molecules. Figure 3b displays a plot of the ratio CCS_g/CCS_0, where CCS_g is the DHSS computed CCS in CO_2 for a cluster ion with g water molecules attached to it. Details on cluster ion structure modeling are again provided in the Supporting Information. For the ions $(HIO_3)IO_3^-$ and $(I_2O_5)_xIO_3^-$ ($x = 1 - 3$), CCS_S/CCS_0 and CCS_g/CCS_0 fall in similar ranges for $g = 5$ and smaller (where CCS_S is the CCS inferred from measurement at saturation ratio S), and for $(I_2O_5)_4IO_3^-$, they fall in similar ranges for $g = 10$ and smaller. This suggests that water vapor sorption does occur to a sufficient extent to complete the reaction $I_2O_5 + H_2O \rightarrow 2HIO_3$ for realistic relative humidity levels, but water vapor sorption beyond the level required for iodic acid formation is limited to only a few water molecules

DOI: 10.1021/acs.jpclett.9b00453
J. Phys. Chem. Lett. 2019, 10, 1935−1941

(i.e., fewer than 20 water molecules). We further remark that despite the apparent sorption of water vapor during mobility measurement, passage through the high-pressure drop mass spectrometer inlet or through the quadrupoles appears to lead to complete loss of excess water. Ions are thus still detected at the mass channel for dehydrated $(I_2O_5)_xIO_3^-$.

Additional quantitative information on the extent of water vapor binding can be gained by comparing observed CCS_S/CCS_0 ratios to a Langmuir-like sorption model[20,40,43]

$$\frac{CCS_S}{CCS_0} = \left[\sum_{g=0}^{\zeta}\left(\frac{P_g}{\left(1 + S\frac{M_{H_2O}n_{sat}}{M_{CO_2}n_{CO_2}}\right)^{-1}\frac{CCS_{g,CO_2}}{CCS_0} + \left(1 + \frac{1}{S}\frac{M_{CO_2}n_{CO_2}}{M_{H_2O}n_{sat}}\right)^{-1}\left(\frac{M_{CO_2}}{M_{H_2O}}\right)^{1/2}\frac{CCS_{g,H_2O}}{CCS_0}}\right)^{-1}\right] \quad (1)$$

$$P_g = \frac{S^g\prod_{j=1}^{g}\left(\frac{\zeta+1}{j} - 1\right)}{1 + \sum_{m=1}^{\zeta}S^m\prod_{j=1}^{m}\left(\frac{\zeta+1}{j} - 1\right)} \qquad g \geq 1 \quad (2)$$

$$P_0 = \frac{1}{1 + \sum_{m=1}^{\zeta}S^m\prod_{j=1}^{m}\left(\frac{\zeta+1}{j} - 1\right)} \quad (3)$$

In eqs 1−3, P_g is the probability that a cluster has g water vapor molecules sorbed, M_{H_2O} and M_{CO_2} are the molecular masses of water and carbon dioxide, respectively, n_{sat} is the water vapor number concentration at saturation, n_{CO_2} is the carbon dioxide number concentration at atmospheric pressure, CCS_{g,CO_2} is the computed CCS of a cluster with g water molecules bound in CO_2 bath gas, and CCS_{g,H_2O} is the computed CCS of a cluster with g water molecules bound in H_2O bath gas. ζ is a fitting parameter representing the maximum number of water vapor molecules that can bind to the cluster ion. The eq 1 calculated average CCS (CCS_S) is required for comparison between model and experiments because the number of water molecules sorbed to a cluster during measurement is not constant; molecules constantly sorb and desorb from a cluster ion. A more complete derivation of these equations is provided in the Supporting Information. Figure 3c displays comparison of the Langmuir model predictions to experimental measurements for selected cluster ions, using fit values of ζ. Results show that the Langmuir model best fits experimental results when ζ exceeds the required number of water vapor molecules needed for completion of the reaction $I_2O_5 + H_2O \rightarrow 2HIO_3$ by 7−14 water molecules. Thus, the modeling approach confirms that iodic acid clusters are only mildly hydrated under atmospherically relevant conditions and not hydrated to a level where ion pairs would wholly or partially dissociate and the clusters would be described as nanodroplets.

In total, our results provide insight into the properties of iodine pentoxide−iodic acid hybrid clusters, similar in chemical composition to those formed in atmospheric nucleation events in coastal regions. IM-MS measurements suggest that such clusters are highly stable, and at atmospherically relevant relative humidities, they can sorb sufficient quantities of water for conversion of most iodine pentoxide to iodic acid. However, sorption of water vapor beyond this level does not appear to be substantial. Combined with similar findings for dimethylamine−sulfuric acid clusters,[21] we suggest that in many circumstances the clusters involved in atmospheric nucleation are only mildly hydrated, and hence, further growth of such clusters hinges upon the interaction between these clusters and the subsequently condensing species (e.g., oxidized organic species). Comparison of measurement inferred CCSs suggests that available computational methods yield structures that capture global structural features of clusters as modeled and measured CCSs are in good agreement. We suggest that further laboratory-scale experiments (e.g., infrared spectroscopy)[44] would be important to probe iodine pentoxide−iodic acid clusters in an effort to develop models describing nucleation events driven by iodine species.

■ ASSOCIATED CONTENT

Supporting Information

The Supporting Information is available free of charge on the ACS Publications website at DOI: 10.1021/acs.jpclett.9b00453.

Descriptions of differential mobility analyzer mass spectrometer measurements, computational approaches used in cluster generation, and IMoS input parameters for collision cross section calculations, as well as derivation of eqs 1−3 (PDF)

Cluster structure coordinates (ZIP)

■ AUTHOR INFORMATION

Corresponding Author

*E-mail: hogan108@umn.edu. Tel.: 1-612-626-8312.

ORCID

Siddharth Iyer: 0000-0001-5989-609X

Notes

The authors declare no competing financial interest.

■ ACKNOWLEDGMENTS

This work was supported by European Research Council Project 692891-DAMOCLES, the Academy of Finland Center of Excellence, ATMATH project, and CSC − Finnish IT Centre.

■ REFERENCES

(1) Sipilä, M.; et al. The Role of Sulfuric Acid in Atmospheric Nucleation. *Science* **2010**, *327*, 1243−1246.

(2) Zhang, R.; Khalizov, A.; Wang, L.; Hu, M.; Xu, W. Nucleation and Growth of Nanoparticles in the Atmosphere. *Chem. Rev.* **2012**, *112*, 1957−2011.

(3) Weber, R. J.; Marti, J. J.; McMurry, P. H.; Eisele, F. L.; Tanner, D. J.; Jefferson, A. Measured Atmospheric New Particle Formation Rates: Implications for Nucleation Mechanisms. *Chem. Eng. Commun.* **1996**, *151*, 53−64.

DOI: 10.1021/acs.jpclett.9b00453
J. Phys. Chem. Lett. 2019, 10, 1935−1941

(4) Dunne, E. M.; et al. Global Atmospheric Particle Formation from CERN CLOUD Measurements. *Science* **2016**, *354* (6316), 1119−1124.
(5) Almeida, J.; et al. Molecular Understanding of Sulphuric Acid-Amine Particle Nucleation in the Atmosphere. *Nature* **2013**, *502*, 359−363.
(6) Kulmala, M.; et al. Direct Observations of Atmospheric Aerosol Nucleation. *Science* **2013**, *339*, 943−946.
(7) Kürten, A.; et al. Neutral Molecular Cluster Formation of Sulfuric Acid-Dimethylamine Observed in Real Time Under Atmospheric Conditions. *Proc. Natl. Acad. Sci. U. S. A.* **2014**, *111*, 15019−15024.
(8) Myllys, N.; Elm, J.; Halonen, R.; Kurtén, T.; Vehkamäki, H. Coupled Cluster Evaluation of the Stability of Atmospheric Acid-Base Clusters with up to 10 Molecules. *J. Phys. Chem. A* **2016**, *120*, 621−630.
(9) Elm, J.; Passananti, M.; Kurtén, T.; Vehkamäki, H. Diamines Can Initiate New Particle Formation in the Atmosphere. *J. Phys. Chem. A* **2017**, *121*, 6155−6164.
(10) Glasoe, W. A.; Volz, K.; Panta, B.; Freshour, N.; Bachman, R.; Hanson, D. R.; McMurry, P. H.; Jen, C. Sulfuric Acid Nucleation: An Experimental Study of the Effect of Seven Bases. *J. Geophys. Res.: Atmos.* **2015**, *120*, 1933−1950.
(11) Kulmala, M.; Petäjä, T.; Ehn, M.; Thornton, J.; Sipilä, M.; Worsnop, D. R.; Kerminen, V. M. Chemistry of Atmospheric Nucleation: On the Recent Advances on Precursor Characterization and Atmospheric Cluster Composition in Connection with Atmospheric New Particle Formation. *Annu. Rev. Phys. Chem.* **2014**, *65*, 21−37.
(12) O'Dowd, C. D.; Jimenez, J. L.; Bahreini, R.; Flagan, R. C.; Seinfeld, J. H.; Hämeri, K.; Pirjola, L.; Kulmala, M.; Jennings, S. G.; Hoffmann, T. Marine Aerosol Formation from Biogenic Iodine Emissions. *Nature* **2002**, *417*, 632−636.
(13) O'Dowd, C. D.; Hoffmann, T. Coastal New Particle Formation: A Review of the Current State-of-the-Art. *Environ. Chem.* **2005**, *2*, 245−255.
(14) Saiz-Lopez, A.; Plane, J. M. C. Novel Iodine Chemistry in the Marine Boundary Layer. *Geophys. Res. Lett.* **2004**, *31*, L04112.
(15) McFiggans, G.; et al. Iodine-Mediated Coastal Particle Formation: An Overview of the Reactive Halogens in the Marine Boundary Layer (RHaMBLe) Roscoff Coastal Study. *Atmos. Chem. Phys.* **2010**, *10*, 2975−2999.
(16) Hoffmann, T.; O'Dowd, C. D.; Seinfeld, J. H. Iodine Oxide Homogeneous Nucleation: An Explanation for Coastal New Particle Production. *Geophys. Res. Lett.* **2001**, *28*, 1949−1952.
(17) Sipilä, M.; et al. Molecular-Scale Evidence of Aerosol Particle Formation via Sequential Addition of HIO_3. *Nature* **2016**, *537*, 532−534.
(18) Lanucara, F.; Holman, S. W.; Gray, C. J.; Eyers, C. E. The Power of Ion Mobility-Mass Spectrometry for Structural Characterization and the Study of Conformational Dynamics. *Nat. Chem.* **2014**, *6*, 281−294.
(19) Hogan, C. J.; Fernandez de la Mora, J. Tandem Ion Mobility-Mass Spectrometry (IMS-MS) Study of Ion Evaporation from Ionic Liquid-Acetonitrile Nanodrops. *Phys. Chem. Chem. Phys.* **2009**, *11*, 8079−8090.
(20) Oberreit, D.; Rawat, V. K.; Larriba-Andaluz, C.; Ouyang, H.; McMurry, P. H.; Hogan, C. J. Analysis of Heterogeneous Water Vapor Uptake by Metal Iodide Cluster Ions via Differential Mobility Analysis-Mass Spectrometry. *J. Chem. Phys.* **2015**, *143*, 104204.
(21) Thomas, J. M.; He, S.; Larriba-Andaluz, C.; DePalma, J. W.; Johnston, M. V.; Hogan, C. J. Ion Mobility Spectrometry-Mass Spectrometry Examination of the Structures, Stabilities, and Extents of Hydration of Dimethylamine-Sulfuric Acid Clusters. *Phys. Chem. Chem. Phys.* **2016**, *18*, 22962−22972.
(22) Larriba, C.; Hogan, C. J. Ion Mobilities in Diatomic Gases: Measurement versus Prediction with Non-Specular Scattering Models. *J. Phys. Chem. A* **2013**, *117*, 3887−3901.
(23) Shrivastav, V.; Nahin, M.; Hogan, C. J.; Larriba-Andaluz, C. Benchmark Comparison for a Multi-Processing Ion Mobility Calculator in the Free Molecular Regime. *J. Am. Soc. Mass Spectrom.* **2017**, *28*, 1540−1551.
(24) Ude, S.; Fernandez de la Mora, J. Molecular Monodisperse Mobility and Mass Standards from Electrosprays of Tetra-Alkyl Ammonium Halides. *J. Aerosol Sci.* **2005**, *36*, 1224−1237.
(25) Gabelica, V. Recommendations for Reporting Ion Mobility Mass Spectrometry Measurements. *Mass Spectrom. Rev.* **2019**, DOI: 10.1002/mas.21585.
(26) Hogan, C. J.; Fernandez de la Mora, J. Ion-Pair Evaporation from Ionic Liquid Clusters. *J. Am. Soc. Mass Spectrom.* **2010**, *21*, 1382−1386.
(27) Ouyang, H.; Larriba-Andaluz, C.; Oberreit, D. R.; Hogan, C. J. The Collision Cross Sections of Iodide Salt Cluster Ions in Air via Differential Mobility Analysis-Mass Spectrometry. *J. Am. Soc. Mass Spectrom.* **2013**, *24*, 1833−1847.
(28) Marti, J. J.; Weber, R. J.; McMurry, P. H.; Eisele, F.; Tanner, D.; Jefferson, A. New Particle Formation at a Remote Continental Site: Assessing the Contributions of SO_2 and Organic Precursors. *J. Geophys. Res.: Atmos.* **1997**, *102*, 6331−6339.
(29) DePalma, J. W.; Bzdek, B. R.; Doren, D. J.; Johnston, M. V. Structure and Energetics of Nanometer Size Clusters of Sulfuric Acid with Ammonia and Dimethylamine. *J. Phys. Chem. A* **2012**, *116*, 1030−1040.
(30) Chen, M.; et al. Acid-Base Chemical Reaction Model for Nucleation Rates in the Polluted Atmospheric Boundary Layer. *Proc. Natl. Acad. Sci. U. S. A.* **2012**, *109*, 18713−18718.
(31) McMurry, P. H.; Li, C. The Dynamic Behavior of Nucleating Aerosols in Constant Reaction Rate Systems: Dimensional Analysis and Generic Numerical Solutions. *Aerosol Sci. Technol.* **2017**, *51*, 1057−1070.
(32) Mason, E. A.; McDaniel, E. W. *Transport Properties of Ions in Gases*; Wiley: New York, 1988.
(33) Zhang, J.; Dolg, M. ABCluster: the artificial bee colony algorithm for cluster global optimization. *Phys. Chem. Chem. Phys.* **2015**, *17*, 24173−24181.
(34) Larriba, C.; Hogan, C. J. Free Molecular Collision Cross Section Calculation Methods for Nanoparticles and Complex Ions with Energy Accommodation. *J. Comput. Phys.* **2013**, *251*, 344−363.
(35) Fernández-García, J.; Fernández de la Mora, J. Electrical Mobilities of Multiply Charged Ionic-Liquid Nanodrops in Air and Carbon Dioxide Over a Wide Temperature Range: Influence of Ion-Induced Dipole Interactions. *Phys. Chem. Chem. Phys.* **2014**, *16*, 20500−20513.
(36) Larriba-Andaluz, C.; Fernandez-Garcia, J.; Ewing, M. A.; Hogan, C. J.; Clemmer, D. E. Gas Molecule Scattering &Ion Mobility Measurements for Organic Macro-Ions in He Versus N_2 Environments. *Phys. Chem. Chem. Phys.* **2015**, *17*, 15019−15029.
(37) Maißer, A.; Thomas, J. M.; Larriba-Andaluz, C.; He, S.; Hogan, C. J., Jr The Mass-Mobility Distributions of Ions Produced by a Po-210 source in Air. *J. Aerosol Sci.* **2015**, *90*, 36−50.
(38) Pepin, R.; Petrone, A.; Laszlo, K. J.; Bush, M. F.; Li, X.; Tureček, F. Does Thermal Breathing Affect Collision Cross Sections of Gas-Phase Peptide Ions? An Ab Initio Molecular Dynamics Study. *J. Phys. Chem. Lett.* **2016**, *7*, 2765−2771.
(39) Kwantwi-Barima, P.; Ouyang, H.; Hogan, C. J.; Clowers, B. H. Tuning Mobility Separation Factors of Chemical Warfare Agent Degradation Products via Selective Ion-Neutral Clustering. *Anal. Chem.* **2017**, *89*, 12416−12424.
(40) Rawat, V. K.; Vidal-de-Miguel, G.; Hogan, C. J. Modeling Vapor Uptake Induced Mobility Shifts in Peptide Ions Observed with Transversal Modulation Ion Mobility Spectrometry-Mass Spectrometry. *Analyst* **2015**, *140*, 6945−6954.
(41) Murray, B. J.; et al. Glass Formation and Unusual Hygroscopic Growth of Iodic Acid Solution Droplets with Relevance for Iodine Mediated Particle Formation in the Marine Boundary Layer. *Atmos. Chem. Phys.* **2012**, *12*, 8575−8587.

DOI: 10.1021/acs.jpclett.9b00453
J. Phys. Chem. Lett. 2019, 10, 1935−1941

(42) Smith, D. K.; Pantoya, M. L.; Parkey, J. S.; Kesmez, M. The Water-Iodine Oxide System: A Revised Mechanism for Hydration and Dehydration. *RSC Adv.* **2017**, *7*, 10183−10191.
(43) Li, C.; Hogan, C. J., Jr. Vapor Specific Extents of Uptake by Nanometer Scale Charged Particles. *Aerosol Sci. Technol.* **2017**, *51*, 653−664.
(44) Waller, S. E.; Yang, Y.; Castracane, E.; Racow, E. E.; Kreinbihl, J. J.; Nickson, K. A.; Johnson, C. J. The Interplay Between Hydrogen Bonding and Coulombic Forces in Determining the Structure of Sulfuric Acid-Amine Clusters. *J. Phys. Chem. Lett.* **2018**, *9*, 1216−1222.

DOI: 10.1021/acs.jpclett.9b00453
J. Phys. Chem. Lett. 2019, 10, 1935−1941